frontiers | Frontiers in Earth Science

TYPE Original Research
PUBLISHED 03 April 2024
DOI 10.3389/feart.2024.1369986

Check for updates

OPEN ACCESS

EDITED BY
Madhavaraju Jayagopal,
National Autonomous University of Mexico, Mexico

REVIEWED BY
Zezhang Song,
China University of Petroleum, China
Bowen Song,
China University of Geosciences Wuhan, China

*CORRESPONDENCE
Yun Liao,
liaoyun553553@163.com

RECEIVED 13 January 2024
ACCEPTED 18 March 2024
PUBLISHED 03 April 2024

CITATION
Zhang J, Liao Y, Lu P, Li W, Zhu K, Li Z, Tian T, Wu J, Sun W, Liu S and Deng B (2024), Three-stage hydrocarbon accumulations in the Middle Permian in the Central Sichuan Basin.
Front. Earth Sci. 12:1369986.
doi: 10.3389/feart.2024.1369986

COPYRIGHT
© 2024 Zhang, Liao, Lu, Li, Zhu, Li, Tian, Wu, Sun, Liu and Deng. This is an open-access article distributed under the terms of the Creative Commons Attribution License (CC BY). The use, distribution or reproduction in other forums is permitted, provided the original author(s) and the copyright owner(s) are credited and that the original publication in this journal is cited, in accordance with accepted academic practice. No use, distribution or reproduction is permitted which does not comply with these terms.

Three-stage hydrocarbon accumulations in the Middle Permian in the Central Sichuan Basin

Jianyong Zhang[1], Yun Liao[2]*, Pengda Lu[2], Wenzheng Li[1], Kedan Zhu[1], Zeqi Li[2], Tengzhen Tian[2], Juan Wu[2], Wei Sun[2], Shugen Liu[2,3] and Bin Deng[2]

[1]PetroChina Hangzhou Research Institute of Geology, Hangzhou, China, [2]College of Energy, Chengdu University of Technology, Chengdu, China, [3]Xihua University, Chengdu, China

The Middle Permain Maokou Formation (P_2m) is a new region of natural gas exploration in the Sichuan Basin, is characterized by bioclastic limestone with localized dolomitization, and karst fractured-vuggy reservoirs. Currently, on the gas source, hydrocarbon accumulation process and control factors in the Sichuan Basin during the Permian are lacking. To bridge this gap, herein, we identified the filling sequence minerals inside the pores/vugs, along with the oil charge of the Maokou Formation using drill cores, thin sections, oil inclusion analysis, and U-Pb dating of calcite cements. The results showed that the reservoir space of the Maokou Formation was predominated by the residual dissolved pores/vugs, fractures, and dissolved fractures. The pores/vugs underwent four stages of mineral filling by very fine-fine (-crystalline, CC1) calcite → fine-medium calcite (CC2: from 256.4 ± 1.7 to 244.1 ± 6.3 Ma) → fibrous calcite (FC; ~183.9 ± 8.2 Ma) → coarse-macro calcite (CC3; ~171.5 ± 5.3 Ma). Combined with the homogenization temperature and salty of fluid inclusion, we considered that three stages of oil charge were present in the Maokou Formation reservoirs. The first stage involved the formation of paleo-oil reservoirs during the Late Permian to Early Triassic, corresponding to the high-maturity aqueous inclusions in CC2, with a homogenization temperature of 106.7°C–137.8°C. At that time, the oil generation from the Lower Cambrian Qiongzhusi Formation rocks peaked, and the generated hydrocarbons migrated upward into the Maokou Formation through the strike-slip faults in the basin center. The second stage involved the formation of paleo-oil reservoirs during the Early Jurassic. The Permian source rocks reached the oil generation window with hydrocarbon expulsion, which was consistent with the oil inclusions in FC. The third stage involved the formation of paleo-gas reservoirs during the Middle Jurassic to Early Cretaceous, corresponding to the high-density methane inclusions and bitumen inclusions occurring in CC3, with the homogenization temperature peaking at 151.9°C–178°C. The natural gas in the Middle Permian of the Central Sichuan Basin is predominantly sourced from the Lower Cambrian Qiongzhusi Formation mudstone and partially from the source rocks of the Middle Permian, indicating a significant

source-reservoir conduit of the strike-slip faults in the basin center. The findings provide considerable baseline data to advance further research in the Sichuan Basin.

KEYWORDS

Sichuan Basin, fluid inclusions, U-Pb dating, oil charge, calcite veins

Introduction

The Permian in the Sichuan Basin, southwest China, is vital formation for exploring and recovering natural gas. 1950s–1980s, The focus of Permian exploration is to search for karst weathering crust reservoir during Indosinian in southern Sichuan, many karst fracture-vuggy gas reservoirs have been discovered successively in the Maokou Formation, e.g., Wolonghe gas-field with a cumulative production volume of 44.13 × 10^8 m (Li et al., 2021; Xiong et al., 2021). Until the 1990s, the discovery of Kaijiang-Liangping trough shifted the exploration focus to the reef-shoals-type gas fields in Upper Permian in northeast Sichuan.

In recent years, high-yield industrial gas flow wells have been obtained in Middle Permian in different synclines and anticlines, such as in Pingluoba, Gaoshiti-Moxi, and Shuangyushi structures in the southwestern, central, and northwestern Sichuan Basin, respectively (Dai et al., 2018; Jiang et al., 2019; Li et al., 2019; Zhang et al., 2020; Li et al., 2023). The Shuangyushi gas field of northwest Sichuan had a controlled reserve of 811.30 × 10^8 m^3 (Shen et al., 2015; Hu, 2019; Yang et al., 2020), showing an excellent prospect of natural gas exploration in the Permian, nevertheless, a major regional breakthrough is still lacking. Many studies have been conducted on the lithofacies paleogeography, reservoir genesis mechanism, distribution law and accumulation process of the natural gas of Permian Maokou Formation in the Sichuan Basin (Hu et al., 2012; Liu et al., 2016; Liu et al., 2018; Yang et al., 2020; Li et al., 2022; Yang et al., 2022), with no knowledge of the gas source, hydrocarbon accumulation process, rules, and control factors (Dong et al., 2017; Dong et al., 2020; Xie et al., 2021).

In recent years, Primary fluid inclusions trapped in cavity cement have been widely used to track the geological fluid charging history of the reservoir and can provide a direct record of the properties of the original geological fluids present at the time of trapping (Bodnar et al., 2014; Liu et al., 2020; Song et al., 2023), and *in situ* U-Pb dating on carbonates via laser-ablation inductively coupled-plasma mass spectrometry (LA-ICP-MS) can determine absolute ages of filled mineral in the reservoir, even if the mineral has a low uranium content (Roberts et al., 2020; Chen et al., 2022; Roberts and Robert, 2022), this provides an opportunity to apply fluid inclusion and U-Pb dating to decipher the timing of the diagenetic history of carbonate reservoir rocks. Herein, We apply LA-ICP-MS U-Pb dating and fluid geochemistry, combined with routine petrography, cathode luminescence. The goal is to determine filling sequence of minerals in the reservoirs from the Middle Permian Maokou Formation in the Central Sichuan Basin. Then the hydrocarbon accumulation process can be determined by fluid inclusions in multistage minerals. The findings provide a basis for further exploration of the Sichuan Basin.

Geological setting

Sichuan Basin is a superimposed basin with multiple stages of tectonic evolution and sea-continent conversion during the Paleozoic. The Permian evolution of the Sichuan Basin has been mainly affected by the expansion-elimination of the Paleo-Tethys Ocean. This stage is considered a vital conversion stage of the Late Paleozoic sedimentary filling and structural development of the Sichuan Basin (Gao et al., 2005). The Caledonian movement and Yunnan movement intensively uplifted the Leshan-Longnvsi area of the Sichuan Basin, which forms the overall paleo-geomorphology of the basin and surroundings, with high elevations in the southwest and low elevations in the northeast, which also resulted in the sedimentary framework of the Permian. Due to the Dongwu movement and Emei taphrogeny, the strata inside the basin exhibited small-scale tectonic uplifting during the Permian Period, and the Emei mantle plume was high around the center of Lijiang-Dali-Panzhihua. The basin at that time was generally extensional and presented an overall sedimentary framework featuring southern uplifting, western rifting, and northern stretching (Yang et al., 2023).

The Permian System in the Sichuan Basin generally consists of the Liangshan, Qixia, Maokou, Longtan, and Changxing formations, while some areas sediment the Emeishan basalts. The Lower Permian Liangshan Formation (P_1l) is predominated by coal-bearing clastic rocks and contains abundant bauxite. The lithology is mainly bauxitic mudstone and shale, with small amounts of sandstone, siltstone, and limestone (Zhang et al., 2012; Huang et al., 2017). Further, due to the underwater paleo-uplift, the Liangshan Formation is generally characterized by gradual thinning from the basin margin to the basin center, except for that in the southwest and southeast margins, which exhibit gradual thickening from the denudation zone to the basin center owing to the tectonic uplifting. The Middle Permian developed the Qixia and Maokou formations, of which the Qixia Formation (P_2q) is predominantly blocky limestone in the central and eastern basin and dolomite with an eye-eyelid structure in the western basin (Figure 1B).

Part of the Maokou Formation (P_2m) is uplifted and denudated, due to the rising of the Emei mantle plume. The sedimentary center is located in the southwest and northwest of Sichuan Basin, and the strata are gradually thinning northeastward (Zhang et al., 2012; Huang et al., 2017). Based on the sedimentary characteristics, the Maokou Formation is divided into four members. The first member of the Makou Formation (Mao-I Member) comprises deep-water ramp deposition of carbonates, associated with sea level rising, and develops the biogentic limestone with the eye-eyelid structure. The deposition of the second and third members of the Maokou Formation (Mao- II and III Members) is accompanied by the gradual falling of the sea level. These two members transition into the shallow-water ramp deposits gradually, and in some regions, into intra-platform shoals. The sedimentary

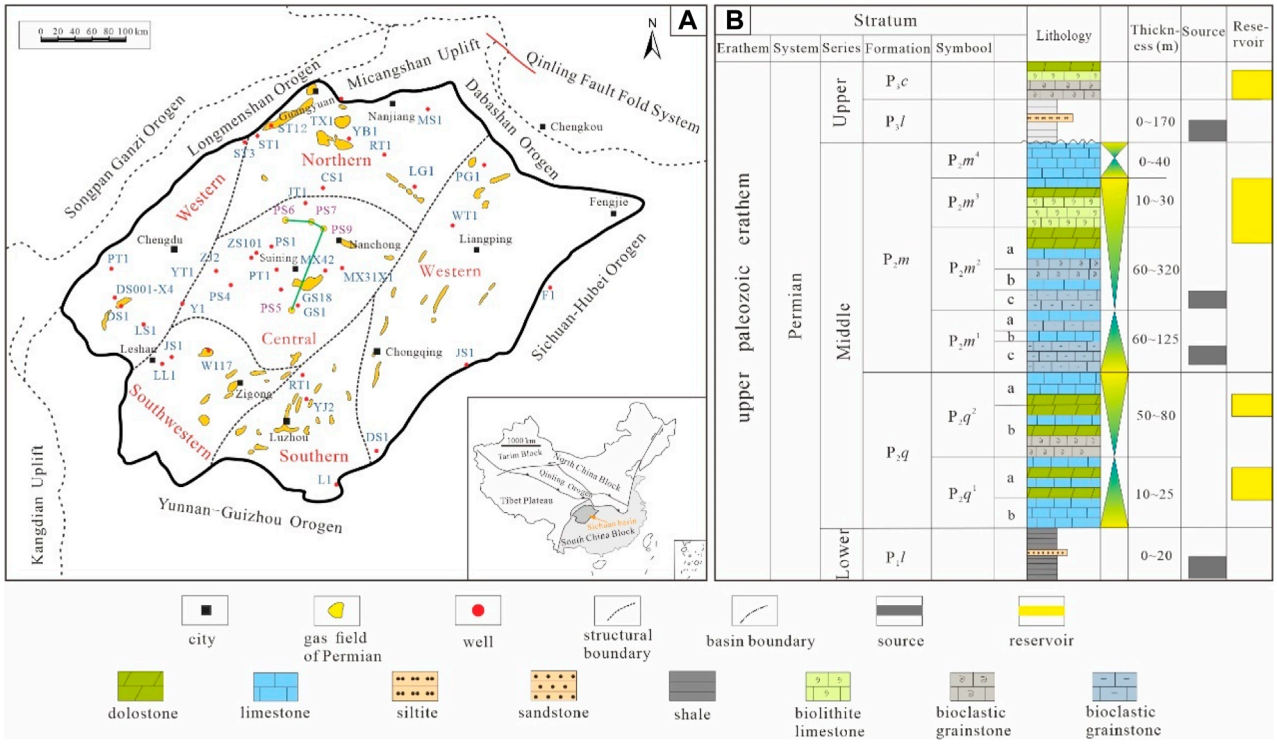

FIGURE 1
Distribution of Permian gas reservoirs and locations of representative wells in Sichuan Basin. **(A)** Distribution of tectonic unit, gas fields and representative wells of Middle Permian of the Sichuan Basin. **(B)** Comprehensive stratigraphic histogram Stratigraphic column of the Permian of Sichuan Basin. Abbreviation: P_1l, Liangshan Formation; P_2q, Qixia Formation; P_2m, Maokou Formation; P_3l, Longtan Formation; P_3c, Changxin Formation.

environment comprises relatively shallow water with high energy. The corresponding lithology is mainly micritic bioclastic limestone with chert bands and some dolomite. The lithology of the fourth member of the Maokou Formation (Mao-IV Member) is mostly dark grey micrite. This stratigraphic layer is better preserved in the South Sichuan. However, it is less thick and is even absent in the East Sichuan-South Sichuan region (Hao et al., 2021). From the southwest to the northeast, the sedimentary environment of the Upper Permian Longtan Formation (P_3l) gradually changes from continental to marine, with increasing depth of the sedimentary water. Consequently, the lithology transitions from sandstone, mudstone with limestone interbeds, and coal seams to grey-dark-grey limestone, with interbeds of siliceous rocks and shale and coal streaks. The last Changxing Formation (P_3c) is mostly bioclastic dolomite and oolitic dolomite of the reef-shoal deposition.

The Middle Permian Series is a vital set of strata for hydrocarbon exploration and developing marine-origin reservoirs in the Sichuan Basin. Affected by the Caledonian paleo-geomorphology, the Sichuan Basin presents an overall sedimentary environment with transgression from east and south toward the Central Sichuan during the early Qixia period; additionally, the deposits overlap the paleo-uplift. During the mid-late Qixia period, the sea level falls. Located in the margin of the Bayan Har Basin, the West Sichuan has medium-water-depth ramp deposition and develops small-area carbonate platform-margin facies. Moreover, the intra-platform grain shoals occur in the periphery of the Central Sichuan paleo-uplift (Bai et al., 2020; Hao et al., 2021). During the mid-late Maokou period, the intra-platform rift occurs from Central Sichuan to North Sichuan, while the platform-margin-carbonate platform facies deposits along the rift edges. The intra-platform high-energy shoals of the Mao-II and III Members mainly occur from Jiange (North Sichuan) to Guang'an (Central Sichuan), West Sichuan, and the margin of the South Sichuan. At the end of the Maokou period, karst paleo-geomorphology is formed with the rising of the mantle plume, and some regions are concealed by volcanic rocks.

The latest exploration results of the Permian natural gas resources in the Sichuan Basin reveal that the significant pay zones are concentrated in the Qixia Formation, Maokou Formation, Emeishan basalts, and Changxing Formation of different regions (multi-layer and cross-region) (Figure 1A). The Qixia Formation reservoir comprises mainly porous dolostones, mostly occurring in the platform-margin belt in the West Sichuan and the intra-platform structural highs around the paleo-uplift in the Central Sichuan. In the Maokou Formation, the large northwest-striking platform-margin belt in Shuangyushi-Wolonghe controls the distribution of the shoal-facies porous dolostones reservoir of the Mao-II Member. The Mao-III Member develops the hydrothermal-origin dolomite reservoir. In contrast, the south and southwest Sichuan develop karst fractured-vuggy limestone reservoirs (Figure 1B). The pyroclastic gas reservoir is developed in west Sichuan Basin near the volcanic vent. Furthermore, multiple stages of the platform-margin biogenic reef-shoal reservoirs in the Changxing

Formation are stacked over each other along the trough sides (Liu et al., 2017; Zhang et al., 2018; Yang et al., 2020; Xie et al., 2021; Yang et al., 2023).

Materials and methods

The samples were collected from the Middle Permian Maokou Formation of Wells PS5, PS6, PS7, and PS9 in the Central Sichuan Basin. CL characteristics were investigated to determine the calcite cement. Fluid inclusion of minerals was analyzed in different stages to understand the hydrocarbon accumulation history. Laser ablation inductively coupled plasma mass spectrometry (LA-ICP-MS) was applied for *in situ* dating of U-Pb to determine the absolute ages of six samples, which developed different stages of calcite cement from Wells PS5, PS7, and PS9. The CL petrography and fluid inclusion thermometry were conducted in the National Key Laboratory of Oil and Gas Reservoir Geology and Exploitation, Chengdu University of Technology, and the calcite *in situ* U-Pb dating was performed in the PetroChina Hangzhou Research Institute of Petroleum Geology.

Petrographic observations: The BK-POL-TR microscope was used to classify the lithology and investigate the microscopic reservoir development characteristics. Moreover, CL imaging was performed using a Leica DM2500 microscope to identify the contact configuration of calcite cement and the filling sequences of rock-forming minerals. The CL8200 MK5, with an operating current of 300 μA at 15 kV was performed at the Chengdu University of Technology.

Fluid inclusion analysis: The LabRam HR Evolution confocal Raman microscope was used to analyze the composition of fluid inclusions. Equipped with a 532-nm green laser, the accessible frequencies reached 0.65 cm^{-1}, and the focal length of the spectrometer was 800 mm. In our research, a 1000-μm confocal hole and a 400-μm slit were used, and the spectral resolution was approximately 1.5 cm^{-1}. To ensure the accuracy of tests, a reference sample of monocrystalline silicon (520.7 cm^{-1}) was used to calibrate the instrument. Raman spectroscopy was performed for different phases inside fluid inclusions, and the specific composition of different fluid inclusions was identified according to the positions of the Raman spectral characteristic peaks. Fluid inclusion microthermometry was performed by Leica DMLP microscope equipped with Linkam THMSG600 heating-freezing stage, in which the temperature could be controlled between −196°C and 600°C, with a post-calibration precision of ±0.1°C. In this study, the cooling/heating rate was set at 10°C/min under normal conditions. When the temperature reached the phase change temperature, the heating and cooling rates were changed to 5°C and 2°C/min, respectively.

U-Pb Dating: Six samples with abundant macro-scale fluid activity were placed in a cylinder (diameter: 1.5–2.5 cm; thickness: approximately 8 mm), cast in epoxy resin, and polished (Figure 2). *In situ* U-Pb dating using LA-ICP-MS was performed at the PetroChina Hangzhou Research Institute of Geology using the IC5 instrument of the radioactive isotope laboratory that can deal with ultra-low content of ^{238}U. We used matrix-matched calcite standards AHX-1a (age: 209.8 ± 1.3 Ma) collected from the Tarim Basin as the primary calibration standard for correction of matrix-related mass bias in the $^{238}U/^{206}Pb$ ratios. The average U concentration of calcite standard AHX-1A is 0.108 ± 0.010 ppm (Chen et al., 2020), and WC-1 (age: 254 ± 6 Ma) (Roberts et al., 2017) were also used for cross-checking of reproducibility. The raw measurements of U/Pb ratios were corrected for elemental fractionation effects using the intercept method and mathematical model method using the Iolite 3.6 software. Subsequently, the data were regressed on Tera-Wasserburg concordia plots using the Isoplot 3.0 software to determine the U-Pb age of each sample.

Results

Petrography

In the Central Sichuan Basin, the reservoir rocks of the Maokou Formation primarily developed in Members II and III of the formation. Eyeball-shaped limestone developed at the bottom of Member II, and gradually deposited micrite blocky bioclastic upward. Localized dolomitization was observed. The dolomite often exhibited subhedral-euhedral crystals with relatively dirty crystal surfaces, and was characterized by "turbid cores and bright rims" (Figure 3I). Member III predominantly developed grey blocky bioclastic grainstone.

The diagenesis of the Maokou Formation in the Central Sichuan Basin has vital effects on the reservoirs property. In the study area, diagenesis was dominated by dissolution and cementation. According to the diagenetic stages, can be divided into contemporaneous, supergene, and burial dissolution (WU, 2019). Due to the Dongwu movement, the Maokou Formation was extensively uplifted and subjected to erosion and karstification to different degrees. Karstification is particularly critical for developing secondary porosity in limestone reservoirs. Further, abundant dissolved fractures, pores, and vugs were observed on the cores of the Maokou Formation. The stylolite was well-developed, indicating intensive pressure-solution. Bitumen was also observed (Figure 3B). The cores of the Permian Maokou Formation in Wells PS5, PS6, PS7, and PS9 showed abundant residual dissolved pores, vugs, and fractures. Still, the fractures and vugs were partially or wholly cemented by calcite (Figure 3A), while some fractures were entirely filled with calcite veins in the cores of Well PS7 (Figures 2G, I). The microscopy results revealed that the millimeter-scale dissolved pores formed by selective dissolution of soluble minerals were completely cemented by multistage calcite (Figure 3C). Further, a fibrous calcite filling fracture was observed in Well PS6 (Figure 3H).

Paragenetic sequence

The four stages of calcite were preliminarily identified by cores, thin sections, and different CL colors. According to the cementation relationship, they can be divided into very fine to fine crystalline calcite (CC1), fine to medium crystalline calcite (CC2), fibrous calcite (FC), and coarse crystalline calcite (CC3). Significant bitumen fillings were associated with the last stage. The high-angle fractures were filled with calcite veins (width: 0.5–1 cm)

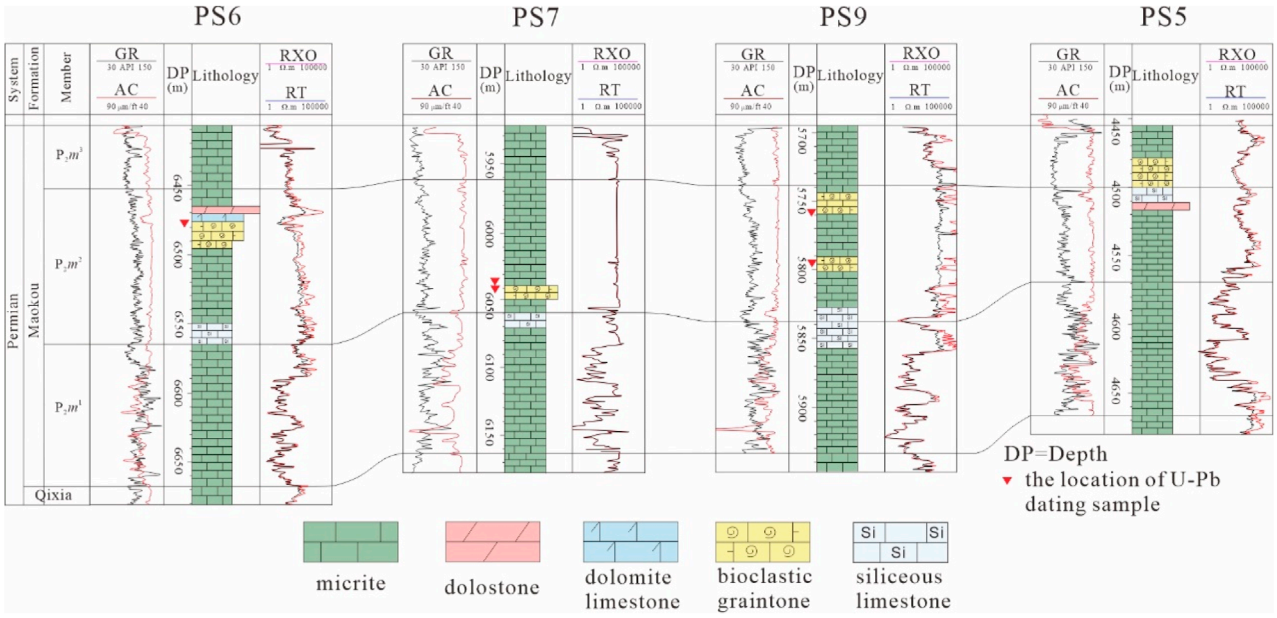

FIGURE 2
A transect showing the lithological features of the Maokou Formation, and U-Pb dating sample location marking (Section position is shown in Figure 1).

(Figures 3C, 4A). In Well PS9, the pores were filled with bitumen and CC3, while in Well PS7, the filling sequence of the fracture was CC1→CC2 (Figures 3F, 4E), followed by bitumen in the fracture center. Some parts of the fractures were entirely filled with FC (Figure 4C), with the width of the calcite vein being 0.2–2.5 cm, and were mainly developed perpendicular to fractures with a crystal width of 0.13–1 mm. The microscopy results revealed calcite zigzag crystal boundaries and relatively clear crystal surfaces. However, no notable cementation sequence could be identified between FC and other stages, and therefore, distinguishing its diagenetic stages was difficult.

Particularly, CL could provide more information on mineral filling sequence characterized with varying Fe and Mn contents. CC1 was characterized by an annular band cemented along the boundary of pores/vugs, subhedral-euhedral with a small grain size, and cloudy crystal surfaces that emitted extremely dark red-light signals under CL (Figures 4E, 5D). This suggested extremely low Fe and Mn contents in the diagenetic fluids, thus indicating a seawater diagenetic environment. The red-light emissions by the crystal edge (bright rim) were associated with the diagenetic process of meteoric water. CC2 was filled inwards along CC1 in a mosaic shape, and the crystal surfaces were relatively clean and exhibited intensive orange-red light under CL (Figures 4E, 5D). This indicated reductive diagenetic fluids, representing a closed seawater environment under shallow burial. CC3 was frequently developed in the centers of pores and vugs. The crystals were coarse with clear and bright crystal surfaces, which emitted dark red light under CL (Figure 5D). These emissions were slightly more intensive than those of CC1. This indicated a semi-open diagenetic environment, with the diagenetic fluids mainly comprising seawater. The CL of FC showed dark red light similar to that of CC3 (Figure 5F).

Fluid inclusion analysis

There were abundant fluid inclusions in the four stages of calcite cement. CC1 presented a predominance of aqueous inclusions that were non-fluorescent under ultraviolet (UV) light. Oil inclusions with blue fluorescence that were elliptical and rod-like in shape in CC2, appeared to be brown under the transmitted light, and ranged in size mainly from 2.5 to 8.3 μm, were distributed randomly and isolated in the crystal, and considered to be primary oil inclusions (Figures 5E, 6D).

Compared with CC2, oil inclusions were less in CC3, and were mostly high-density methane inclusions and bitumen inclusions (Figures 5F, 6C). High-density methane inclusions were distributed in bands, while the bitumen inclusions were distributed in groups. Bitumen inclusions were square, and their size range was mainly 4–12.5 μm. Further, high-density methane inclusions and oil inclusions with blue-green fluorescence were observed in FC. However, the fluid inclusions in CC1 and FC were too small to test.

The composition of the fluid inclusions with different phases was analyzed through laser Raman spectrums. The oil inclusions in CC2 were dominated by liquid hydrocarbons of saturated hydrocarbons, and its typical Raman peak was observed at 2,250 cm^{-1} (Figures 6B, 7A). Moreover, three stable Raman peaks occurred at 1,437, 2,890, and 2,850 cm^{-1} (Figure 7B), implying that n-alkanes with carbon numbers over 10 were in the oil inclusions.

The liquid-phase fluid inclusions in CC3 featured two typical Raman peaks at 2,910.4 and 2,911.8 cm^{-1}. The main component was methane. The inclusion of solid bitumen exhibited characteristic doublet D-G band peaks at 1,360 and 1,620 cm^{-1}.

The homogenization temperatures and melt temperatures of fluid inclusion in CC2 and CC3 were measured to recover the formation temperature and the salinity of the pore water solution in

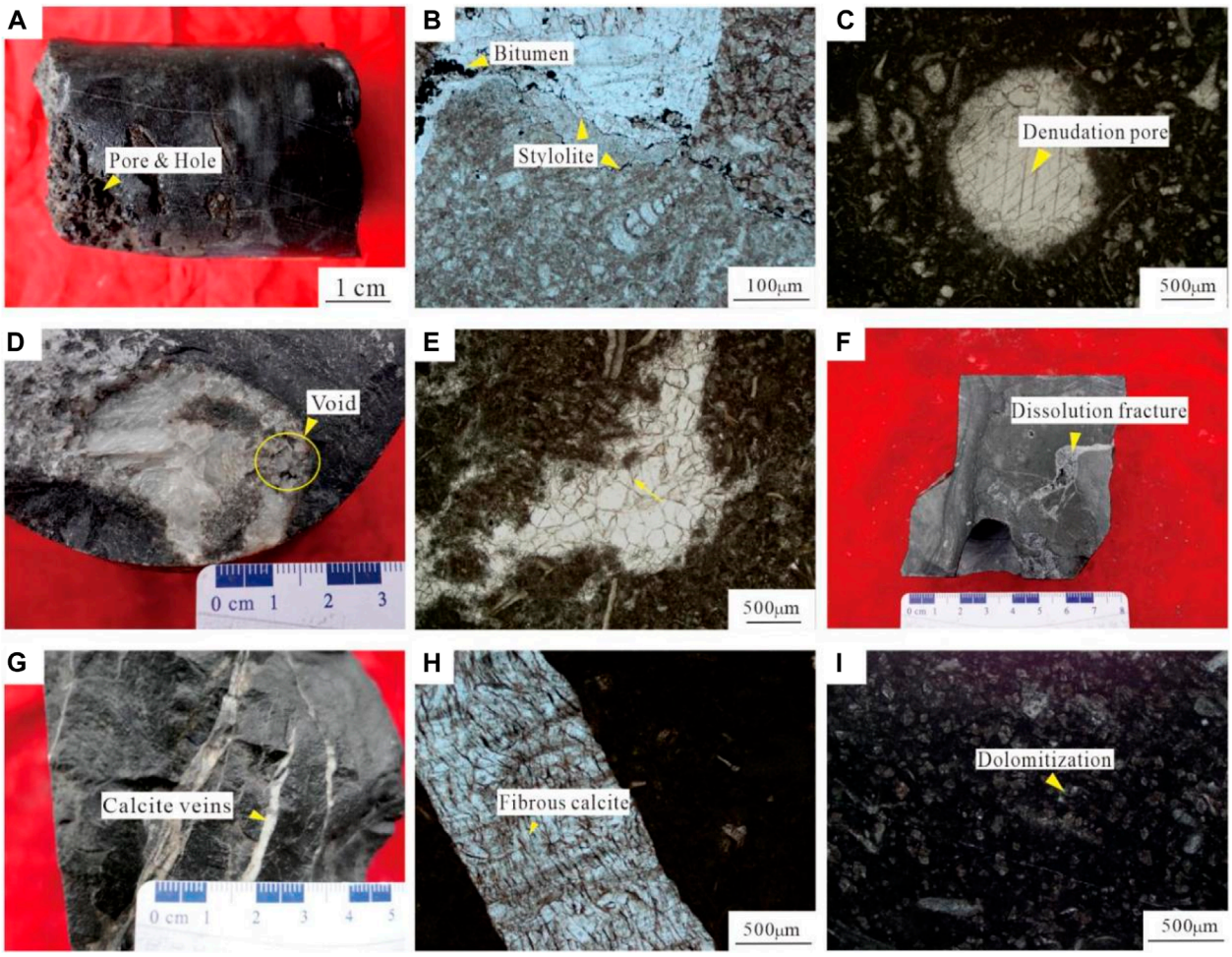

FIGURE 3
Characteristics of the Permian reservoirs in the Central Sichuan Basin. **(A)** Well PS6: 6,475.31 m, well-developed vuggy porosity. **(B)** Well PS6: 6,478.50 m, well-developed multi-stage stylolite, with the bitumen distributed along it; **(C)** Well PS9: 5,760.72 m, calcite filling dissolved pores in the bioclastic limestone. **(D)** Well PS9: 5,748.91 m, the dissolution fracture is not fully filled. **(E)** Well PS9: 5,796.68 m, calcite completely filling the dissolved fracture. **(F)** Well PS9: 5,743.23 m, dissolved fracture; **(G)** Well PS7: 6,037.05 m, calcite vein; **(H)** Well PS6: 6,490.33 m, fibrous calcite filling the structural fracture. **(I)** Well PS6: 6,491.17 m, dolomitization with turbid cores and clear rims.

diagenesis. Homogenization temperatures of the aqueous inclusions in CC2 ranged from 106.7°C to 137.8°C (average: 122.74°C), and peaked at 120°C–130°C. The corresponding Tm values range from −8.1 to −2.3°C. The aqueous inclusion in CC3 exhibited high Th temperature (151.9°C–178.0°C, average: 164.7°C), peaking at 165°C–170°C, while the Tm values ranged from −21.9 to −10.9°C. The modified empirical correlation between the freezing temperature and salinity for an H2O-NaCl system (BODNAR, 1993) was used to calculate the fluid salinity based on the Tm value and has been illustrated in Figure 8. The salinity ranged from 3.76 to 11.83 wt.% NaCl equivalent in CC2 (average: 8.38 wt.%) and from 8.38 to 23.61 wt.% NaCl equivalent in CC3 (average: 16.67 wt.%).

In situ U-Pb dating of carbonate mineral

In total, six samples (one host rock, three CC2, one CC3, and one FC), were dated using LA-ICP-MS U-Pb dating (Supplementary Table S1). The calcite samples were all characterized by low Pb and U contents. U-Pb ages of three analyzed calcite samples of CC2 in the central Sichuan Basin were 244.1 ± 6.3, 256.4 ± 1.7, and 245.2 ± 9.8 Ma, respectively. The MSWD was relatively low (3.1 ≤MSWD ≤6.4), while the U content in the three CC2 samples was 0.476–2.154, 0.442–4.494 and 0.002–6.24 ppm, respectively, with the respective averages of 1.066, 2.214, and 1.13 ppm, while the $^{238}U/^{206}Pb$ ratios were 22.601–25.979, 22.678–25.289, and 0.474–26.233 (Figures 8C, D). The wide range of U-Pb ratios of a single sample allowed highly precise age data with 2σ errors better than 5%, We consider this date as reliably constraining the absolute timing of cementation in the limestone vugs. The U content of the surrounding rock sample was 1.976–5.45 ppm (average: 3.904 ppm). The wide range of $^{238}U/^{206}Pb$ ratio of the samples was 14.892–23.509. The age at the lower intersection point of the Tera-Wasserburg reverse concordia plot was 269.2 ± 2.5 Ma, and the initial $^{207}Pb/^{206}Pb$ value at the upper intersection point was 0.59, with a mean square of the weighted deviates (MSWD) of 4.3 (Figure 9A). In terms of the FC

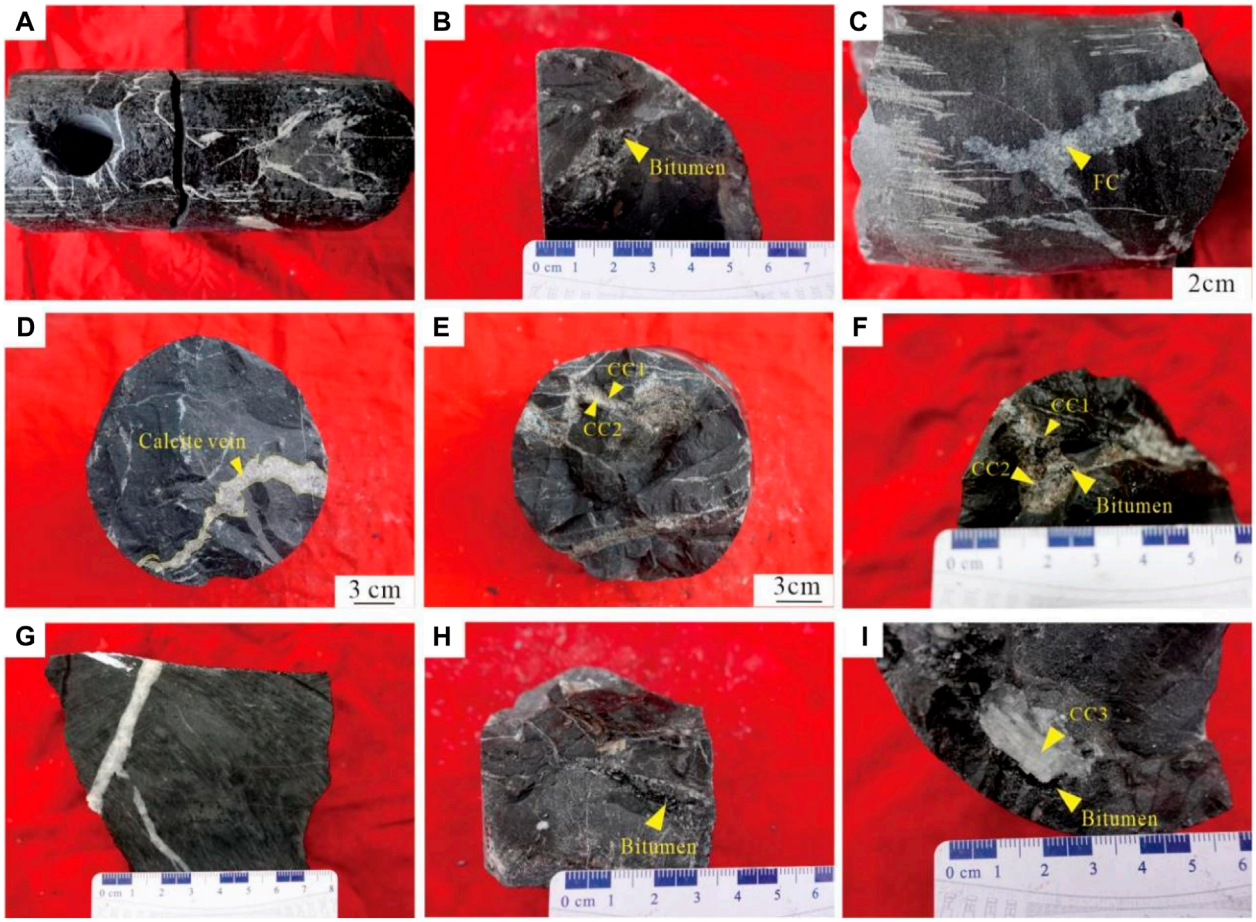

FIGURE 4
Multi-stage fluid activity characteristics of the Middle Permian Maokou Formation reservoir in the Central of Sichuan Basin. **(A)** Well PS6, 6,490.17 m, P_2m^2, calcite veins. **(B)** Well PS9: 5,744.69 m, P_2m^2, voids have been partly filled bitume. **(C)** Well PS6, 6,478.50 m, P_2m^2, fibrous calcite. **(D)** Well PS7, 6,039.47 m, P_2m^2. **(E,F)** Well PS7, 6,045.64 m, P_2m^2, calcite fillings of CC1 and CC2 stages, bitume in the center. **(G)** Well PS7, 6,044.98 m, P_2m^2, calcite vine. **(H)** Well PS9, 5,744.47 m, P_2m^2, walls of dissolved fractures lined with calcite cement, and residual space fully filled with bitumen. **(I)** Well PS9, 5,744.47 m, P_2m^2, CC3 and bitumen fillings in vugs.

samples, the U content was 0.006–0.226 ppm (average: 0.081 ppm), $^{238}U/^{206}Pb$ ratio was 2.737–30.784, and U-Pb age of the calcite sample was 183.9 ± 8.2 Ma, with MSWD = 3.8 (Figure 9F). Finally, the U content of the CC3 sample was 0.06–3.701 ppm (average: 0.953 ppm), while the $^{238}U/^{206}Pb$ ratio ranged from 15.498 to 36.192 and the U-Pb age was 171.5 ± 5.3 Ma, with MSWD = 3.8 (Figure 9E).

Discussion

Diagenesis

Barker (1990) reported a correlation among the density, salinity, and temperature of solutions that could reflect the diagenetic fluid environment at that time. As indicated by the temperature-salinity-density plot of fluid inclusions (Figure 10), the fluid density of the fluid inclusions of CC2 and CC3 in the Maokou Formation in the Central Sichuan Basin was 1.01–1.08 g/cm^3. For the low-salinity inclusions in CC2, the homogenization temperature was not correlated with salinity, perhaps due to the relatively open environment in which the early inclusions were formed. During the early diagenetic stage, the stratum burial temperature was relatively low, the environment was relatively open, and fluid exchange was frequent; additionally, the salinity of the formation fluids may be reduced by dilution.

For the high-salinity inclusions in the later-formed CC3, the homogenization temperature was positively correlated with salinity. With the deepened burial and elevated formation temperature, the fluid environment was relatively closed, with fewer effects of extraneous fluids, and hence, the salinity of the formation fluids increased, which reflects the burial diagenetic evolution process of the Maokou Formation in the Central Sichuan Basin that can be characterized by an increase in the formation temperature, a shift in the diagenetic environment from open to closed, and maturity of organic content increasing with increasing burial.

The short penecontemporary stage occurred after the deposition of Maokou Formation, which was in a seawater diagenetic environment. CC1 was distributed as a girdle along the boundary of the dissolved pore/fracture, and was enriched with Mg-Fe and lean for Mn. It demonstrated weak luminescence under CL and mainly

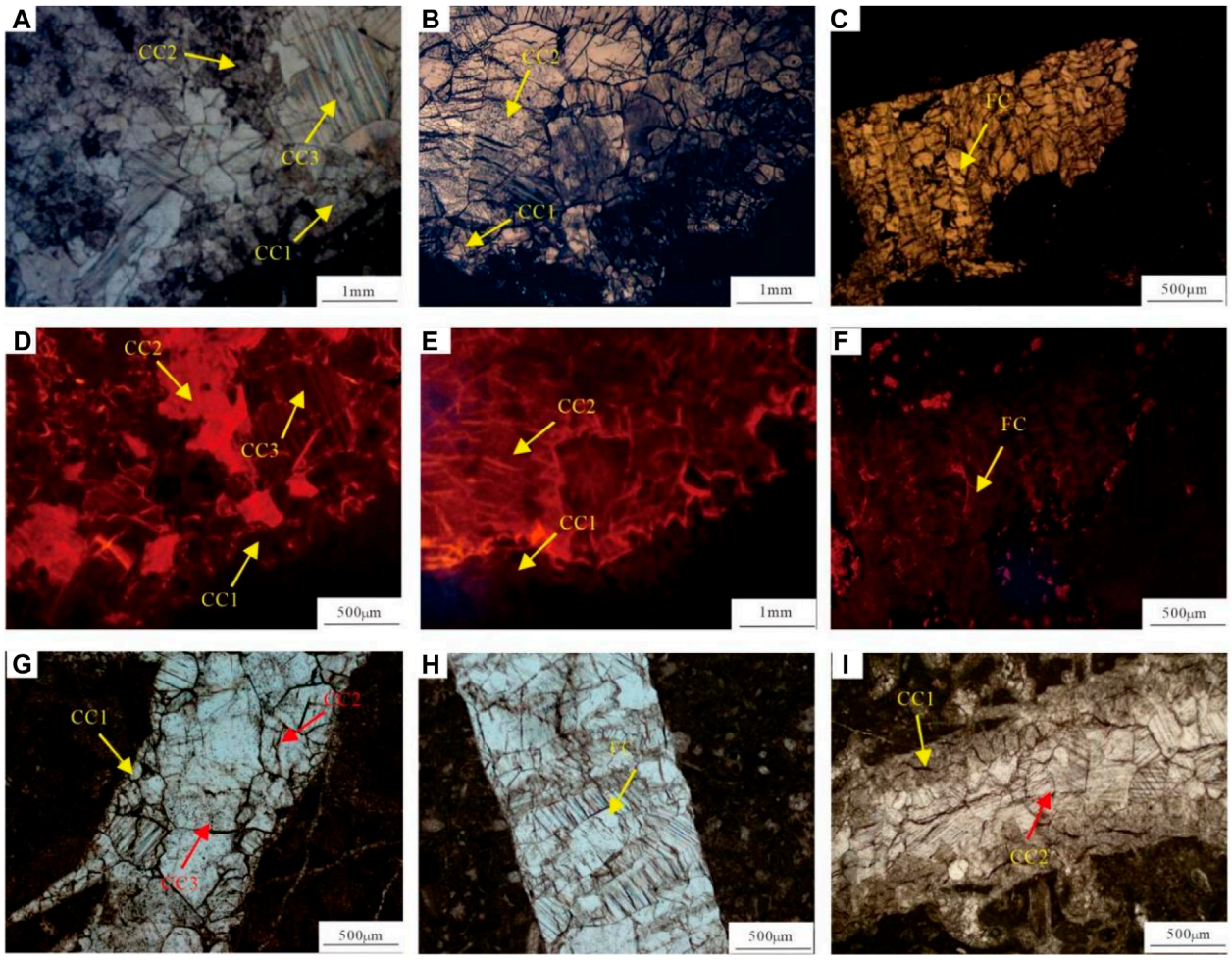

FIGURE 5
Filling sequence of mineral cement in the Permian reservoirs in the Central Sichuan Basin. **(A)** Well PS7, 6,037.23 m, P_2m^2. **(B)** Well PS9, 5,743.0 m, P_2m^2. **(C)** Well PS6, 6,478.50 m, P_2m^2. **(D)** CL imaging of **(A)**. **(E)** CL imaging of **(B)**. **(F)** CL imaging of **(C)**. **(G)** Well PS7, 6,041.89 m, P_2m^2. **(H)** Well PS6, 6,491.17 m, P_2m^2. **(I)** Well PS7, 6,037.06 m, P_2m^2.

consisted of unstable aragonite and high-magnesium calcite. The calcite at this stage commonly exhibited luminous rims, possibly because of the near-surface and shallow-burial environment of freshwater or mixed water during early diagenesis. By the late stage of the Middle Permian, the formation underwent stretching and uplifting due to the Dongwu movement. The Maokou Formation was uplifted and subjected to exposure, during which leaching and dissolution of fresh water along the formed tensile fractures resulted in abundant karst vugs and dissolved fractures.

During the Late Permian, the Maokou Formation entered the shallow-medium burial stage, during which CC2 occurred as inlays along CC1 and occupied relatively more reservoir space toward the centers of pores/fractures. Due to the diagenetic process related to freshwater, CC2 had higher Fe and Mn content and presented intensive orange-red luminescence under CL (Figures 4E, 5B). At that time, the majority of CC1 was fully dissolved, which was manifested as the core characteristic that the CC2 filled the dissolved fracture along the margin (Figure 4D). The karst system provided migration channels for hydrothermal fluids as well as freshwater and seawater during the initial deposition of the Longtan Formation. The dolomite distribution also presented characteristics that were related to the early dissolution fractures (Figure 3B). LIU H. et al. (2016) analyzed the diagenetic fluids of subhedral-euhedral fine dolomite of the Maokou Formation in Central Sichuan. They reported that the dolomite was mainly of hydrothermal origin and occurred in a closed reductive environment. Concerning FC genesis, it is widely believed that FC is the product of the drainage of the geological fluids due to the ultra-high tectonic overpressure during the same tectonic stage (ZHANG et al., 2014).

The fractures filled by FC were mostly structural fractures with straight sections. U-Pb dating of FC suggested that the calcite veins were formed during the Yanshanian movement, due to the over-saturation of pore fluids after the fracture opening was triggered. During the mid-late diagenetic stage, the Maokou Formation of Central Sichuan developed CC3, which occurred in the centers of pores and fractures and exhibited large crystals. Moreover, it presented extremely weak luminescence under CL and was

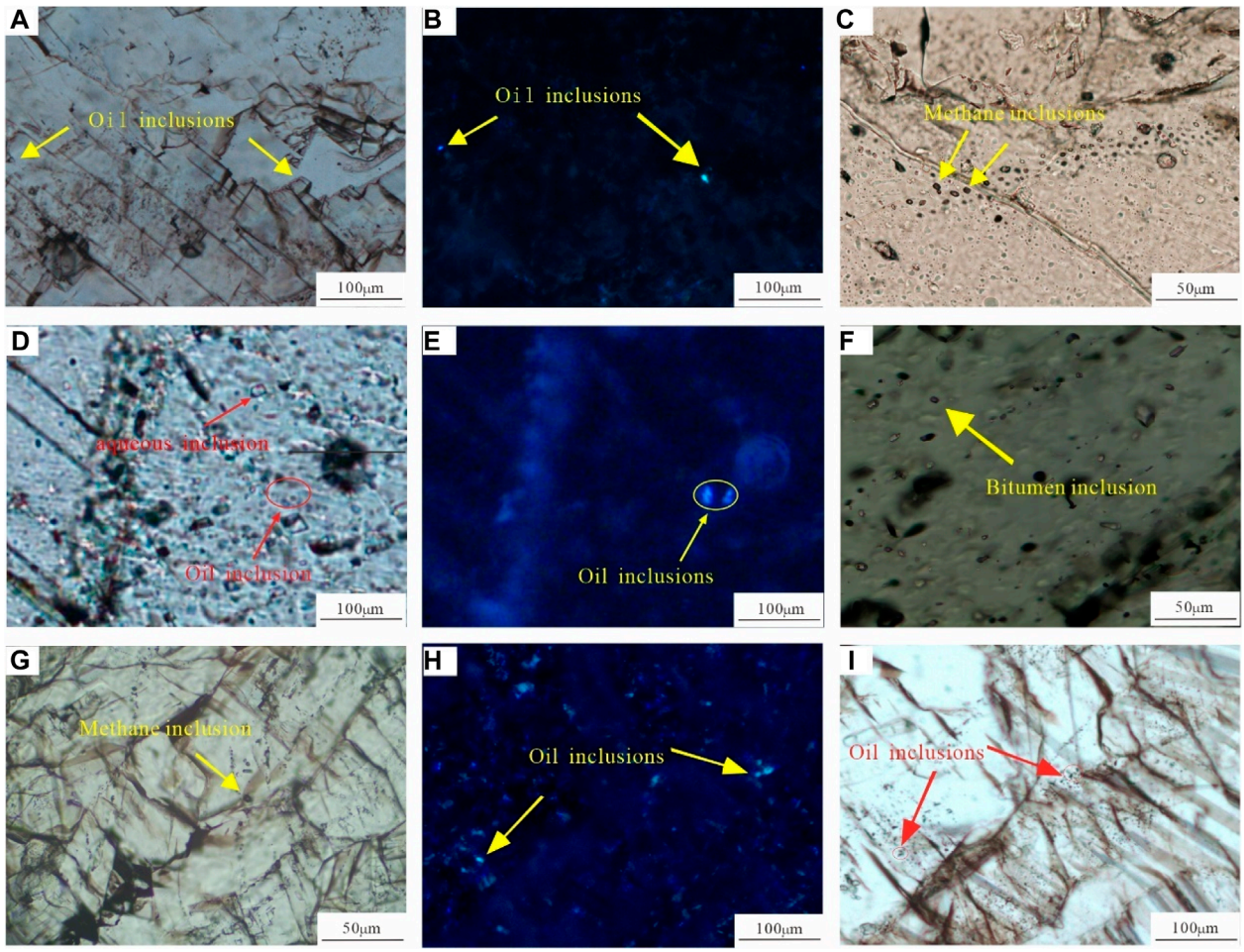

FIGURE 6
Characteristics of fluid inclusions of different stages in the Permian reservoirs in the Central Sichuan Basin. **(A,B)** Well PS6, P_2m^2, 6,478.65 m, oil inclusions in CC2. **(C)** Well PS9, P_2m^2, 5,760.72 m, methane inclusions in CC3. **(D,E)** Well PS7, P_2m^2, 6,037.06 m, oil inclusions in CC2. **(F)** Well PS6, P_2m^2, 6,491.17 m, bitumen inclusions in CC3. **(G)** Well PS6, P_2m^2, 6,478.65 m, methane inclusions in FC. **(H,I)** Well PS6, P_2m^2, 6,491.17 m, oil inclusions in FC.

derived from the diagenetic fluids of seawater. The residual pores of such cement were often filled with bitumen, formed during the main hydrocarbon accumulation of Maokou reservoirs. This bitumen resulted from the thermal cracking of crude oil during deep burial.

According to the above analysis, the diagenetic evolution of the pores and fractures can be roughly divided into six stages. (1) During the penecontemporaneous stage, CC1 is deposited along the pre- and fracture boundary and stacked toward the centers of pores and fractures. (2) In the supergene stage, karst led to the development of fracture and cave, deep hydrothermal fluids migrates along the karst and fracture, and dolomitization also occurs. (3) CC2 is deposited along CC1 and stacked over each other toward the centers of pores/fractures, and part of CC1 is completely dissolved. (4) Crude oil accumulates in the remaining reservoir space. (5) During the Early Jurassic, part of the overpressure fluids in the pore migrates through fractures to form FC veins. (6) During the mid-late diagenetic stage, CC3 was deposited. With the deepened burial, crude oil gradually cracks, and the remaining reservoir space is filled with solid bitumen.

Natural gas accumulation in P_2m in the Penglai gas area

The homogenization temperature of the fluid inclusions was combined with the regional burial-thermal evolution history (Figure 11). According to the U-Pb dating of samples and fluid inclusion compositional characteristics, the hydrocarbon accumulation sequence of the Middle Permian Maokou Formation in the Central Sichuan Basin was identified. The formation had three stages of hydrocarbon emplacement.

Due to the Emei taphrogeny during the Late Permian to Early Triassic, the Central Sichuan Basin was subjected to constant stretching and subsidence and started to receive deposits again. The source rocks of the Middle Permian were approximately 3,700 m deep, with a formation temperature of 80°C–100°C. The maturity of P_2 source rocks ranged from 0.5% to 0.7%, and mainly generated low-maturity oil. Contrastingly, the source rocks of the Lower Cambrian Qiongzhusi Formation were buried approximately 4,500 m deep at the mature stage, with Ro values in the range of 1.0%–1.5%, at the stage of massive oil generation.

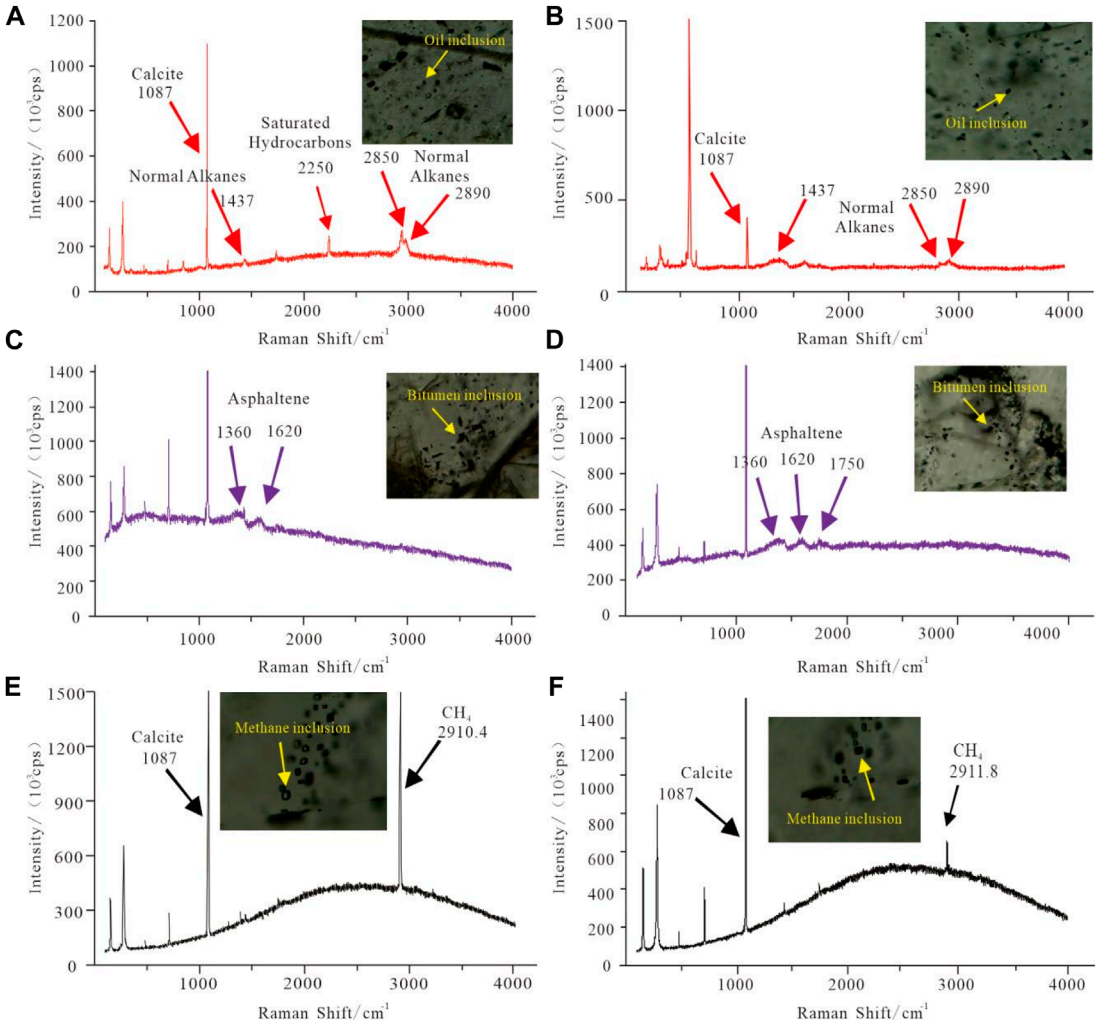

FIGURE 7
Laser Raman spectral characteristics of the Permian reservoirs in the Central Sichuan Basin. **(A)** Well PS6, 6,491.33 m. **(B)** Well PS6, 6,490.33 m. **(C)** Well PS7, 6,041.89 m. **(D)** Well PS7, 6,041.89 m. **(E)** Well PS5, 4,481.89 m. **(F)** Well PS5, 4,481.89 m.

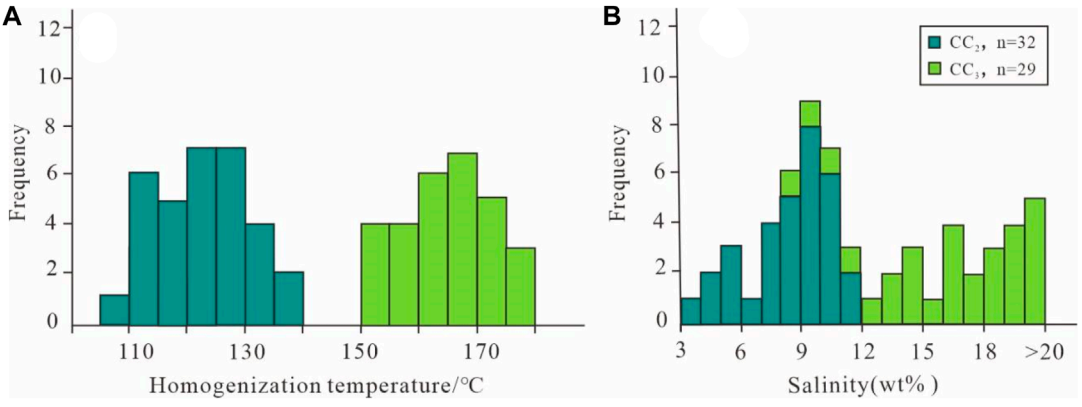

FIGURE 8
Homogenization temperature **(A)** and salinity **(B)** frequency of inclusions in rock-forming minerals of the Middle Permian Maokou Formation in the Central Sichuan Basin.

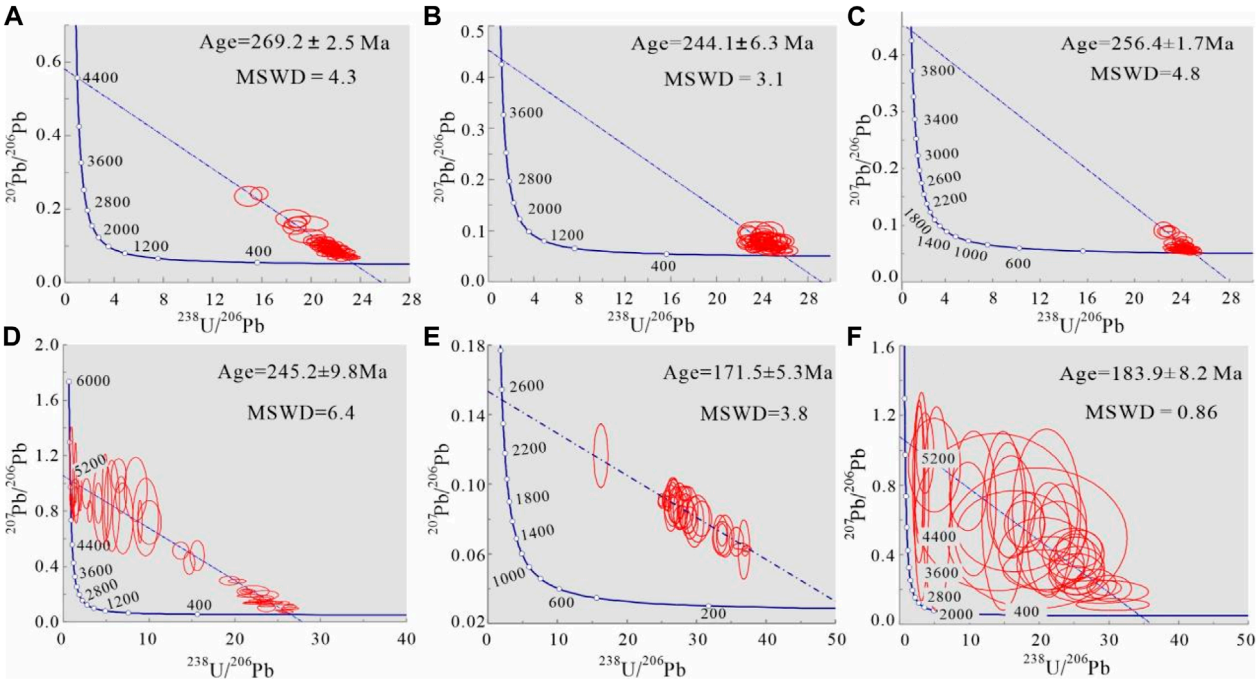

FIGURE 9
U-Pb dating plots of rock-forming minerals of different stages in the Middle Permian Maokou Formation in the northern slope of Central Sichuan Basin. **(A)** Host rock of Well PS7, P_2m^2, 6,041.14 m. **(B)** CC2, Well PS7, P_2m^2, 6,041.14 m. **(C)** CC2, Well PS7, P_2m^2, 6,039.47 m. **(D)** CC2, Well PS9, P_2m^2, 5,760.72 m. **(E)** CC3, Well PS9, P_2m^2, 5,796.68 m. **(F)** FC, Well PS6, P_2m^2, 6,478.65 m.

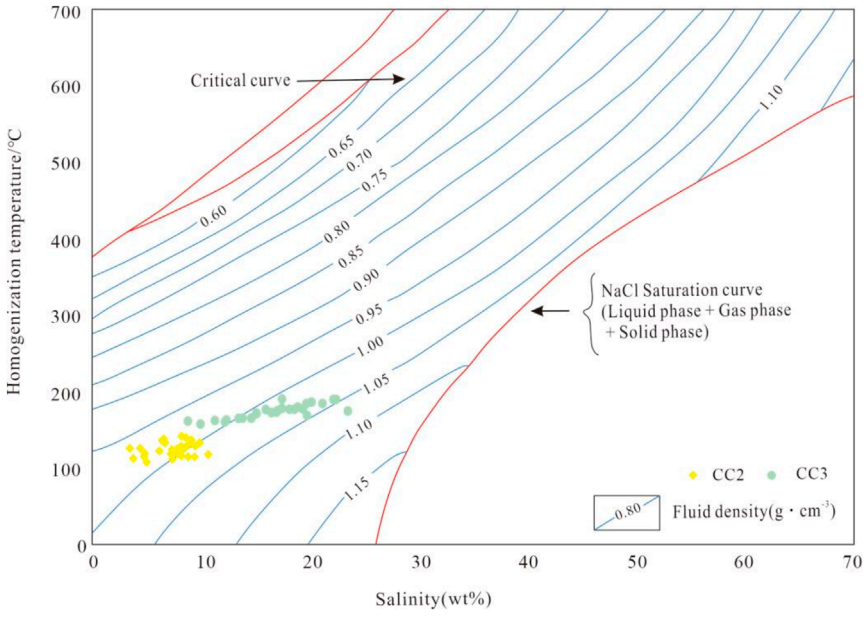

FIGURE 10
T-W-ρ plot of fluid inclusions in the P_2m^2 reservoir.

U-Pb dating of CC2 and its high-maturity blue fluorescence oil inclusions indicated that during the Late Permian to Early Triassic, the crude oil, which was generated by the Lower Cambrian Qiongzhusi Formation, migrated upward into the Middle Permian Maokou reservoirs via the strike-slip fault, and corresponded to the aqueous inclusions with the homogenization temperature of 106.7°C–137.8°C in CC2. Furthermore, the current reservoir appraisal and gas content evaluation of some wells in the

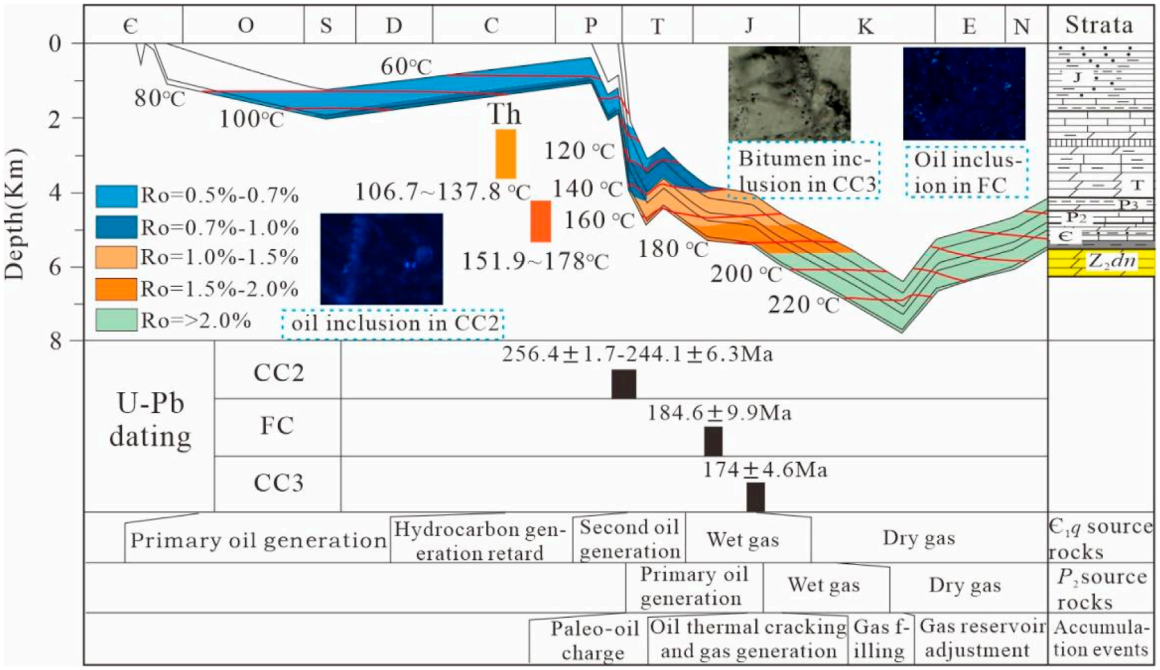

FIGURE 11
Hydrocarbon accumulation events of P_2 in the Penglai gas area. Histogram of fluid inclusion homogenization temperatures and calcite time estimated from U–Pb dating are also shown for comparison with the ambient temperatures.

Gaoshiti-Moxi area revealed the distribution of gas-producing wells along the fault.

FC (183.9 ± 8.2 Ma) was formed during the Early Jurassic, and the maturity of source rocks of P_2 ranged from 1.0% to 1.5%, suggesting that the mature stage was associated with hydrocarbon expulsion. The oil inclusions in FC were indicative of the second stage of oil charge. CC3 was dominated by bitumen inclusions and high-density methane inclusions, demonstrating the capturing of oil-cracking gas. The Lower Cambrian Qiongzhusi source rocks enter the high-maturity gas-generating stage during the Middle Jurassic to Cretaceous. During the Late Jurassic to Early Cretaceous, the Middle Permian source rocks mainly produce wet gas. With the constantly deepened burial, these source rocks reached the over-mature stage by the Early Cretaceous and started to generate a massive amount of dry gas. Meanwhile, *in situ* cracking occurred in the early-formed paleo-oil reservoirs.

The Paleozoic of the Central Sichuan Basin developed three sets of source rocks, namely the Upper Permian Longtan Formation, Middle Permian marlstone, and Lower Cambrian Qiongzhusi Formation mudstone (Liu et al., 2018). The carbon isotopes of ethane are an essential criterion to identify natural gas types (Sun et al., 2021). The carbon isotope ratio of ethane in the Central Sichuan Basin was less than 29‰, which is a characteristic of oil-type gas (Figure 12A). Therefore, the coal-bearing system of the Upper Permian Longtan Formation was eliminated as a possible gas source. The correlation diagram of $\ln(C_1/C_2)$ and $\ln(C_2/C_3)$ indicated that the gas was derived from oil cracking (Figure 12B).

The isotope characteristics of natural gas in the Middle Permian of the Central Sichuan Basin were similar to those of the Longwangmiao Formation, which originated from the Qiongzhusi Formation. This implied that the natural gas in the Middle Permian also originated from the Qiongzhusi Formation mudstone. Some samples presented high values of $\delta^{13}C_1$, indicating the possible contributions of the source rocks in the Middle Permian itself. Compared with the natural gas of the Sinian Dengying Formation which originated from the source rocks of Qiongzhusi Formation, the natural gas in the Middle Permian showed a lower $\delta^{13}C_2$ value and partial distribution reversal of carbon isotopes of methane and ethane (the carbon isotopes of methane and ethane of the Dengying Formation exhibited positive distributions). This was because of the different contributions of gas related to crude oil cracking.

In previous studies, biomarker indexes, such as regular sterane, Ts/Tm, and gammacerane/C_{31} homohopane, were used to track bitumen sources in the Middle Permian reservoirs in the Central Sichuan Basin. The biomarker characteristics of the reservoir bitumen were more similar to those of the Qiongzhusi Formation mudstone and instead differentiated from those of the Upper and Middle Permian marlstone (Dong et al., 2020). The carbon isotope characteristics of natural gas and biomarker characteristics of the reservoir bitumen indicated that the natural gas in the northern slope of the Central Sichuan paleo-uplift? was mainly oil-cracking gas, which was mostly derived from the Qiongzhusi Formation mudstone and partially from the Middle Permian source rocks.

The Central Sichuan Basin has undergone multiple stages of tectonic movements. The early oblique stretching during the early Caledonian movement and the extrusion stress in late Caledonian formed the basis of the current structural style of the Central Sichuan. In the late Hercynia, under the influence of the Emei rift movement, the central Sichuan Basin was in an NE-SW stretching stress environment. Under the action of oblique tension,

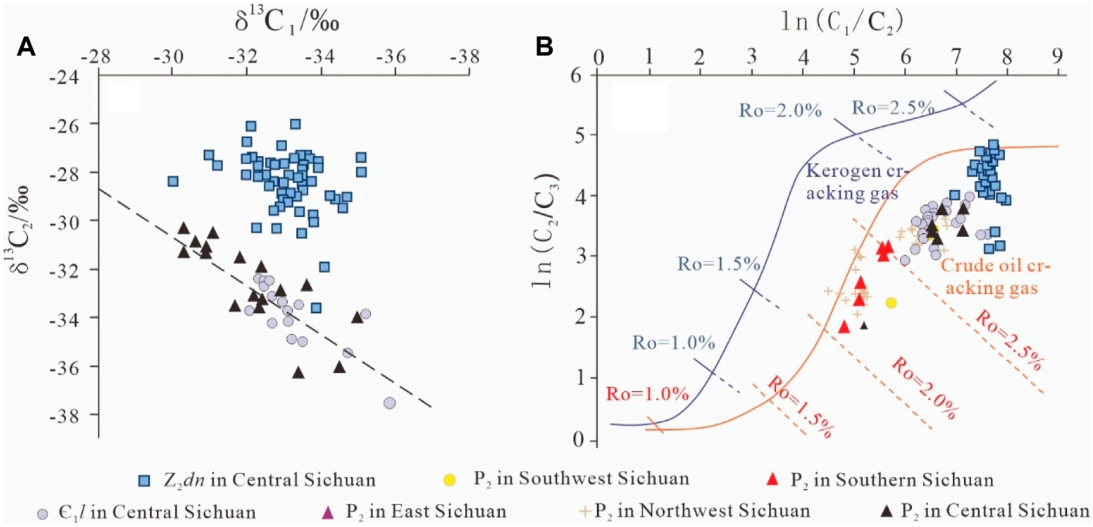

FIGURE 12
Carbon isotope characteristics of natural gas in different layers **(A)**, and $\ln(C_1/C_2)$ vs. $\ln(C_2/C_3)$ of natural gas **(B)** in the Permian in sichuan Basin.

the main faults of early Caledonian were activated and formed normal faults with certain strike-slip components in the Permian (He et al., 2005; Luo et al., 2012). Extensive studies have been performed on the development characteristics of the strike-slip fault in Central Sichuan (Ma et al., 2018; Jiao et al., 2021; Guan et al., 2022). These strike-slip faults are steep and do not cross the Triassic gypsum-salt rocks. Significant strike-slip faults can serve as excellent fluid migration channels connecting multiple upper and lower layers. These can connect gas sources and promote the upward migration of the deep Lower Cambrian hydrocarbons to the Middle Permian carbonate reservoirs. Moreover, faulting can promote the formation of extensive fractured-vuggy reservoir rocks and is significant for improving the reservoir physical properties and stimulating hydrocarbon migration. In many places, such as the Tarim Basin in China, oil and gas reservoirs are related to strike-slip structures; additionally, the intensity of strike-slip faulting directly affects hydrocarbon enrichment (Deng et al., 2021).

The burial-thermal evolution history of the Central Sichuan suggests that the U-Pb dating of CC2 corresponds to the thermal maturity of the Middle Permian marlstone source rocks (0.5%–0.7%; low-maturity). Therefore, the oil inclusions with blue fluorescence in CC2 cannot be derived from the Middle Permian source rocks. Instead, they should be derived from the Lower Cambrian Qiongzhusi Formation. During the Late Permian, the strata subsided rapidly, and the Qiongzhusi Formation entered the oil generation window again. By the Early Triassic, it peaked at hydrocarbon generation, and the crude oil entered into and accumulated at the Maokou Formation reservoirs through the faults to form paleo-oil reservoirs. During the Early Jurassic, the Middle Permian source rocks started the second-stage oil emplacement, and during the Middle Jurassic, the paleo-oil reservoirs started oil cracking; further, by the Cretaceous, the source rocks of the Qiongzhusi Formation and Middle Permian reached the over-mature stage, and the crude oil in the paleo-oil reservoirs changed into the paleo-gas reservoirs with abundant bitumen, after nearly complete oil cracking. The large strike-slip faults of the inheriting development in the northern slope of the Central Sichuan could well connect the upper and lower layers, which vertically resulted in hydrocarbon accumulation association of multiple Permian layers charged by the Upper Sinian and Lower Cambrian (Figure 13).

Conclusion

In this study, the filling sequence of minerals inside the pores/vugs and the oil charge of the Maokou Formation were identified. The main findings are as follows:

(1) The reservoir space of the Middle Permian Maokou Formation in the Central Sichuan Basin is predominated by dissolved fractures and pores/vugs, part of which is filled with fibrous calcite, fine-medium calcite, and bitumen. The filling sequence was CC1 → CC2 → FC → CC3 → Bitumen.

(2) The different types of cements considerably differentiated the types and phases of fluid inclusions. During the Late Permian to Early Triassic, the maturity of Middle Permian source rocks reached 0.5%. Therefore, the high-maturity oil inclusions in CC2 indicated the hydrocarbon emplacement from the Lower Cambrian Qiongzhusi Formation. The high-density methane inclusions and bitumen inclusions trapped in CC3 indicate the Middle Jurassic gas generation via oil cracking.

(3) The Middle Permian Maokou Formation in the Central Sichuan Basin has undergone three stages of hydrocarbon emplacement, which are the formation of a paleo-oil reservoir via hydrocarbon emplacement of crude oil generated by the Lower Cambrian Qiongzhusi Formation during the Late

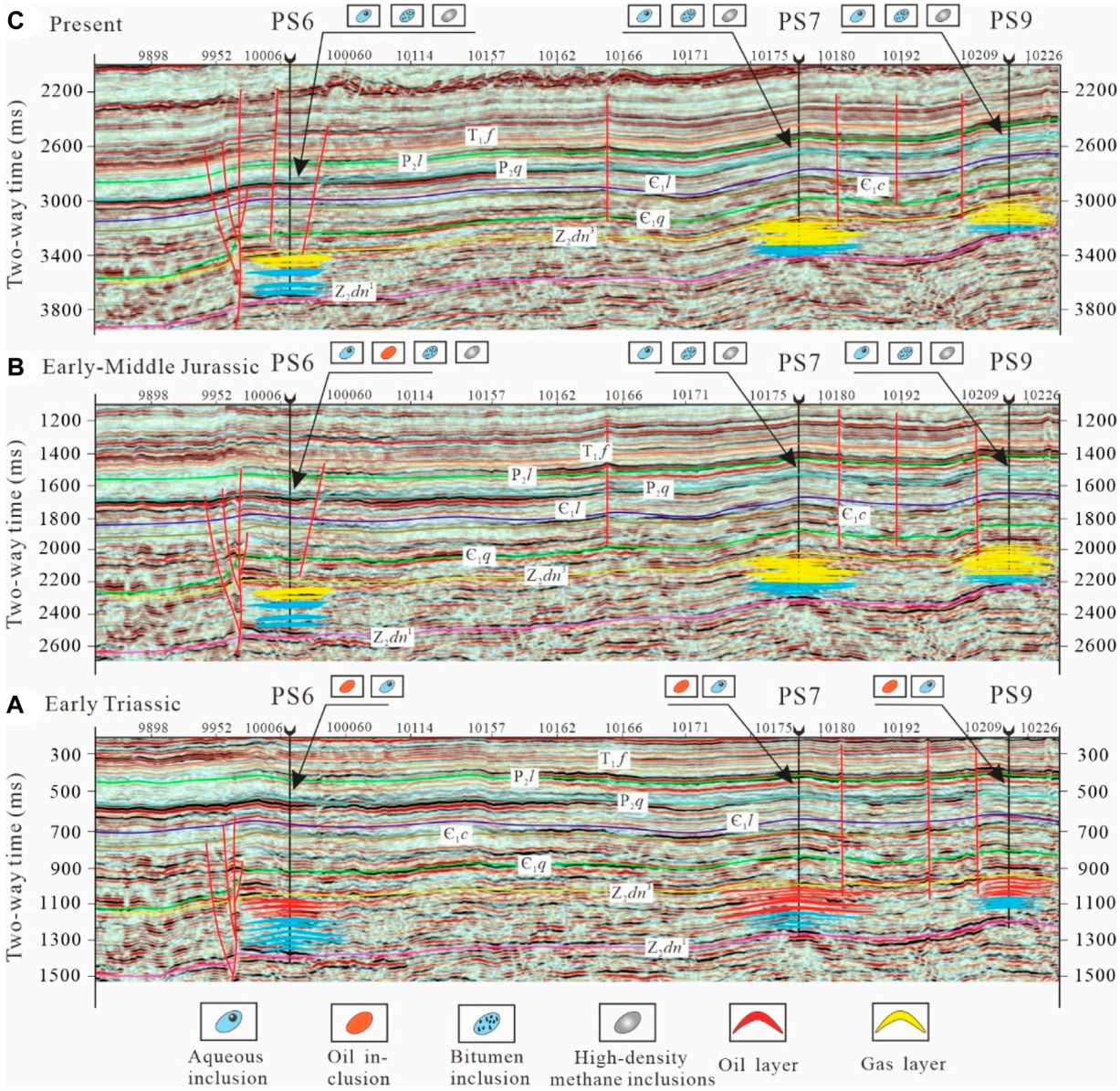

FIGURE 13
Hydrocarbon accumulation and evolution pattern of the Middle Permian in the Central of Sichuan Basin. ((**A**) Oil inclusions and aqueous inclusions are developed in the Maokou Formation during early Triassic, (**B**) The inclusions are mainly high-density methane with a small amount of oil inclusions during early-middle Jurassic, (**C**) Almost all are methane inclusions in present). The location of the profiles can be seen in Figure 1.

Permian to Early Triassic. The second oil was charged by the Middle Permian source rocks during the Early Jurassic and gas reservoirs formed via oil reservoir cracking during the Middle Jurassic to Early Cretaceous. The natural gas in the Central Sichuan Basin mainly was source from the Qiongzhusi Formation mudstone, with some amount sourced from the Middle Permian source rocks, as indicated by the natural gas carbon isotope characteristics and bitumen biomarker characteristics.

Overall, the study provides vital information to advance exploration in the Sichuan Basin.

Data availability statement

The original contributions presented in the study are included in the article/Supplementary Material, further inquiries can be directed to the corresponding author.

Author contributions

JZ: Conceptualization, Methodology, Writing–original draft, Writing–review and editing, Funding acquisition, Resources.

YL: Conceptualization, Methodology, Writing–original draft, Writing–review and editing, Formal Analysis, Validation. PL: Data curation, Investigation, Validation, Writing–review and editing. WL: Data curation, Validation, Writing–review and editing. KZ: Project administration, Resources, Writing–review and editing. ZL: Investigation, Supervision, Writing–review and editing. TT: Data curation, Methodology, Writing–review and editing. JW: Formal Analysis, Validation, Writing–review and editing. WS: Methodology, Validation, Writing–review and editing. SL: Funding acquisition, Project administration, Writing–review and editing. BD: Project administration, Supervision, Writing–review and editing.

Funding

The author(s) declare that financial support was received for the research, authorship, and/or publication of this article. This research was funded by the China National Petroleum Corporation Science and Technology Major Project (No.2023ZZ16YJ01), the Key Project of Natural Science Foundation of China (No.U19B6003).

Conflict of interest

The authors declare that the research was conducted in the absence of any commercial or financial relationships that could be construed as a potential conflict of interest.

Publisher's note

All claims expressed in this article are solely those of the authors and do not necessarily represent those of their affiliated organizations, or those of the publisher, the editors and the reviewers. Any product that may be evaluated in this article, or claim that may be made by its manufacturer, is not guaranteed or endorsed by the publisher.

Supplementary material

The Supplementary Material for this article can be found online at: https://www.frontiersin.org/articles/10.3389/feart.2024.1369986/full#supplementary-material

References

Bai, X. L., Chi, C., He, Y., et al. (2020). Sequence stratigraphic characteristics and sedimentary evolution model of the middle permian Qixia Formation in the Sichuan Basin. *J. northeast petroleum Univ.* 44 (06), 33–42. doi:10.3969/j.issn.2095-4107.2020.06.004

Bodnar, R. J. (1993). Revised equation and table for determining the freezing point depression of H2O-Nacl solutions. *Geochim. Cosmochim. Acta* 57 (3), 683–684. doi:10.1016/0016-7037(93)90378-a

Bodnar, R. J., Lecumberri-Sanchez, P., Moncada, D., and Steele-MacInnis, M. (2014). 13.5 - fluid inclusions in hydrothermal Ore Deposits. *Treatise Geochem.* 13, 119–142.

Chen, J. X., Guo, X. W., Tao, Z., Cao, Z., Wang, B., Zhang, X., et al. (2022). U-Pb dating of oil charge in superimposed basins: a case study from the Tarim Basin, NW China. *GSA Bull.* 134 (11-12), 3176–3188. doi:10.1130/b36324.1

Chen, T., Zhao, J. X., Feng, Y. X., Pan, W., and Liu, D. (2020). <italic>*In-situ*</italic> LA-MC-ICPMS U-Pb dating method for low-uranium carbonate minerals. *Chin. Sci. Bull.* 65 (Z1), 150–154. doi:10.1360/tb-2019-0355

Dai, J. X., Ni, Y. Y., Qin, S. F., Huang, S. P., Peng, W. L., and Han, W. X. (2018). Geochemical characteristics of ultra-deep natural gas in the Sichua Basin, SW China. *Petroleum Explor. Dev.* 45, 588–597. doi:10.11698/PED.2018.04.05

Deng, S., Liu, Y. Q., Liu, J., et al. (2021). Structural styles and evolution models of intracratonic strike-slip faults and the implications for reservoir exploration and appraisal: a case study of the shunbei area, Tarim Basin. *Geotect. Metallogenia* 45 (06), 1111–1126. doi:10.16539/j.ddgzyckx.2020.05.015

Dong, C. Y., Liu, M. C., Li, D. J., et al. (2020). Gas source tracing of lower permian in gaoshiti-moxi area, Sichuan Basin. *Fault-Block Oil&Gas Field* 27 (03), 273–277. doi:10.6056/dkyqt202003001

Dong, C. Y., Xie, Z. Y., Zhu, H., et al. (2017). New insight for gas source and gas accumulation modes of middle permian in central Sichuan Basin. *J. Xi'an Shiyou Univ. Sci. Ed.* 32 (04), 18–23+31. doi:10.3969/j.issn.1673.-064X.2017.04.003

Gao, C. L., Huang, Z. G., Ye, D. L., et al. (2005). Three paleo-oceans in the early paleozoic and their control to basin China. *Petroleum Geol. Exp.* (05), 19–28.

Guan, S. W., Liang, H., Jiang, H., et al. (2022). Characteristics and evolution of the main strike-slip fault belts of the central Sichuan Basin, southwestern China, and associated structures. *Earth Sci. Front.* 29 (06), 252–264. doi:10.13745/j.esf.Sf.2022.8.8

Hao, Y., Yao, Q. Y., Tian, H., et al. (2021). The affective neuroscience of socioeconomic status: implications for mental health - CORRIGENDUM. *Mar. Orig. Pet. Geol.* 30 (01), 1–10. doi:10.1192/bjb.2021.99

He, B., Xu, Y. G., Wang, Y. M., et al. (2005). Nature of the Dongwu movement and its temporal and spatial evolution. *Earth Sci.* (01), 89–96.

Hu, D. F. (2019). Breakthrough in natural gas exploration in the platform margin shoal at the Maokou Fm in the Yuanba area, Sichuan Basin, and its implications. *Nat. Gas. Ind.* 39 (03), 1–10. doi:10.3787/j.issn.1000-0976.2019.03.001

Hu, M. Y., Hu, Z. G., Wei, G. Q., et al. (2012). Sequence lithofacies paleogeography and reservoir prediction of the Maokou Formation in Sichuan Basin. *Petroleum Explor. Dev.* 39 (01), 45–55.

Huang, H. Y., He, D. F., Li, Y. Q., et al. (2017). The prototype and its evolution of the Sichuan sedimentary basin and adjacent areas during Liangshan and Qixia stages in Permian. *Acta Petrol. Sin.* 33 (04), 1317–1337.

Jiang, Y. Q., Zhou, Y. D., Chen, Z. Y., et al. (2019). Sedimentary pattern and exploration significance of Permian reefs and shoals in intra-platform depressions, eastern Sichuan Basin. *Nat. Gas. Geosci.* 30 (11), 1539–1550. doi:10.11764/j.issn.1672-1926.2019.08.008

Jiao, F. Z., Yang, Y., Ran, Q., et al. (2021). Distribution and gas exploration of the strike–slip faults in the central Sichuan Basin. *Nat. Gas. Ind.* 41 (08), 92–101. doi:10.3787/j.issn.1000-0976.2021.08.009

Li, L. L., Luo, K. P., Liu, X., et al. (2023). Controlling effect of Late Paleozoic tectonic and sedimentary differentiation on multi-type gas reservoirs in Permian, Sichuan Basin. *Pet. Geology&Experiment* 45 (01), 60–71. doi:10.11781/sysydz202301060

Li, R. R., Yang, X., Zhang, Y., et al. (2019). Characteristics and high-yield model of gas reservoirs of permian Qixia Formation, Shuangyushi area, northwestern Sichuan Basin. *Nat. Gas Explor. Dev.* 42 (04), 19–27. doi:10.12055/gaskk.issn.1673-3177.2019.04.003

Li, R., Su, C. P., Jia, H. P., et al. (2022). Reservoir characteristics and genesis of dolomite of middle permian Qixia Formation in southwestern Sichuan Basin. *Lithol. Reserv.* 34 (04), 103–115. doi:10.12108/yxyqc.20220410

Li, T., Zhu, D., Yang, M. L., Zhang, X. H., Li, P., Lu, C., et al. (2021). Early-stage marine dolomite altered by hydrothermal fluids in the middle permian Maokou Formation in the eastern Sichuan Basin, southern China. *Mar. Petroleum Geol.* 134, 105367. doi:10.1016/j.marpetgeo.2021.105367

Liu, D. D., Zhang, C., Pan, Z. K., Huang, Z., Luo, Q., Song, Y., et al. (2020). Natural fractures in carbonate-rich tight oil reservoirs from the Permian Lucaogou Formation, southern Junggar Basin, NW China: insights from fluid inclusion microthermometry and isotopic geochemistry. *Mar. Petroleum Geol.* 119 (104500), 104500–110279. doi:10.1016/j.marpetgeo.2020.104500

Liu, J. Q., Zhen, H. F., Liu, B., et al. (2017). Characteristics and genetic mechanism of the dolomite in the middle permian Maokou Formation, central sichuan area. *Acta Pet. Sin.* 38 (04), 386–398. doi:10.7623/syxb201704003

Liu, S. G., Sun, W., Li, Z. W., et al. (2016a). Distribution characteristics of marine carbonate reservoirs and their tectonic controlling factors across the

Sichuan superimposed basin. *Lithol. Reserv.* 28 (05), 1–18. doi:10.3969/j.issn.1673-8926.2016.05.001

Liu, H., Han, S., Ye, M., Wu, S., Ma, C., Liu, C., et al. (2018a). Medium to large gas fields in Sichuan Basin: distribution characteristics and exploration prospects. *Nat. Gas Explor. Dev.* 41 (02), 55–63. doi:10.1016/j.expneurol.2018.04.013

Liu, H., Ma, T., Tan, X. C., Zeng, W., Hu, G., Xiao, D., et al. (2016b). Origin of structurally controlled hydrothermal dolomite in epigenetic karst system during shallow burial: an example from Middle Permian Maokou Formation, central Sichuan Basin, SW China. *Petroleum Explor. And Dev.* 43 (06), 1000–1012. doi:10.1016/s1876-3804(16)30117-3

Liu, W., Qiu, N. S., Xu, Q. C., et al. (2018b). The quantitative evaluation of the pressurization caused by hydrocarbon generation in the Cambrian Qiongzhusi Formation of the Gaoshiti-Moxi area, Sichuan Basin. *Petroleum Sci. Bull.* 3 (03), 262–271. doi:10.12055/gaskk.issn.1673-3177.2018.02.008

Luo, Z. L., Sun, W., Han, J. H., et al. (2012). Effect of Emei mantal plume on the condition of Permian accumulation in middle-upper Yangtze Area. *Earth Sci. Front.* 19 (06), 144–154.

Ma, D. B., Wang, Z. C., Duan, S. F., Gao, J., Jiang, Q., Jiang, H., et al. (2018). Strike-slip faults and their significance for hydrocarbon accumulation in Gaoshiti–Moxi area, Sichuan Basin, SW China. *Petroleum Explor. And Dev.* 45 (05), 851–861. doi:10.1016/s1876-3804(18)30088-0

Roberts, N. M. W., Drost, K., Matthew, S. A. H., Condon, D. J., Chew, D., Drake, H., et al. (2020). Laser ablation inductively coupled plasma mass spectrometry (LA-ICP-MS) U–Pb carbonate geochronology: strategies, progress, and limitations. *Geochronology* 2 (1), 33–61. doi:10.5194/gchron-2-33-2020

Roberts, N. M. W., Rasbury, E. T., Parrish, R. R., Smith, C. J., Horstwood, M. S. A., and Condon, D. J. (2017). A calcite reference material for LA-ICP-MS U-Pb geochronology. *G-cubed* 18, 2807–2814. doi:10.1002/2016gc006784

Roberts, N. M. W., and Robert, E. H. (2022). Timescales of faulting through calcite geochronology: a review. *J. Struct. Geol.* 158 (104578), 0191–0203. doi:10.1016/j.jsg.2022.104578

Shen, P., Zhang, J., Song, J. R., Hong, H., Tang, D., Wang, X., et al. (2015). Significance of new breakthrough in and favorable targets of gas exploration in the Middle Permian system, Sichuan Basin. *Nat. Gas. Ind.* 35 (07), 391–398. doi:10.1016/j.ngib.2015.09.014

Song, Y. F., Chen, Y., Wang, M., Steele-MacInnis, M., Ni, R., Zhang, H., et al. (2023). In-situ cracking of oil into gas in reservoirs identified by fluid inclusion analysis: theoretical model and case study. *Mar. Petroleum Geol.* 147 (105959), 105959–110277. doi:10.1016/j.marpetgeo.2022.105959

Sun, X., Wang, J., Tao, C., et al. (2021). Evaluation of geochemical characteristics and source of natural gas in Lower Paleozoic, Daniudi area, Ordos Basin. *Petroleum Geol. Exp.* 43 (02), 307–314. doi:10.11781/sysydz202102307

Wu, Y. (2019). *Study on the characteristics of karst reservoir in Chuanzhong area of Sichuan basin[D]*. Xi'an: Xi'an Shiyou University.

Xie, J. R., Li, Y., Yang, Y. M., et al. (2021b). Main controlling factors and natural gas exploration potential of Permian scale volcanoclastic reservoirs in the western Sichuan Basin. *Nat. Gas. Ind.* 41 (03), 48–57. doi:10.3787/j.issn.1000-0976.2021.03.006

Xie, Z. Y., Wei, G. Q., Li, J., et al. (2021a). Geochemical characteristics and accumulation pattern of gas reservoirs of the Sinian-Permian in central Sichuan uplift zone, Sichuan Basin. *China Pet. Explor.* 26 (06), 50–67. doi:10.3969/j.issn.1672-7703.2021.06.004

Xiong, X. X., Chen, R., Yuan, Y., et al. (2021). Seismic prediction of karst reservoirs of the Maokou Formation in Wolonghe structure of Sichuan Basin. *Acta Pet. Sin.* 42 (06), 724–735. doi:10.7623/syxb202106003

Yang, Y. M., Yang, Y., Wen, L., et al. (2020). New exploration progress and prospect of Middle Permian natural gas in the Sichuan Basin. *Nat. Gas. Ind.* 40 (07), 10–22. doi:10.3787/j.issn.1000-0976.2020.07.002

Yang, Y., Wen, L., Chen, C., et al. (2023). Oil and gas expliration potential of the Permian multi-stage platform-margin zone, western Sichuan Basin. *Earth Sci. Front.* 30 (01), 1–10. doi:10.13745/j.esf.sf.2022.8.22

Yang, Y., Wen, L., Song, Z. Z., et al. (2022). Breakthrough and potential of natural gas exploration in multi-layer system of Penglai gas area in the north of central Sichuan paleo-uplift. *Acta Pet. Sin.* 43 (10), 1351–1368+1394. doi:10.7623/syxb202210001

Zhang, B. J., Yin, H., Li, R. R., et al. (2020). New breakthrough of natural gas exploration in the Qixia Formation of middle permian by well pingtan 1 in the southwestern Sichuan Basin and its implications. *Nat. Gas. Ind.* 40 (07), 34–41. doi:10.3787/j.issn.1000-0976.2020.07.004

Zhang, Q. M., Jiang, X. S., Qin, J. H., et al. (2012). Lithofacies palaeogeography of the early Middle Permian Liangshan Formation in northern Guizhou-southern Chongqing area and its bauxite ore-forming effect. *Geol. Bull. China* 31 (04), 558–568.

Zhang, Y. N., Li, R. X., and Liu, H. Q. (2014). A review of fibrous calcite veins and tectonic fluids. *Geol. Sci. Tecnology Inf.* 33 (04), 12–18.

Zhang, Y. N., Li, R. X., and Liu, H. Q. (2018b). A review of fibrous calcite veins and tectonic fluids. *Geol. Sci. Technol. Inf.* 3 (03), 262–271. doi:10.3787/j.issn.1000-0976.2018.01.002